Published in final edited form as:

Cancer Res. 2021 August 15; 81(16): 4332–4345. doi:10.1158/0008-5472.CAN-21-0590.

CDK6 is a therapeutic target in myelofibrosis

Avik Dutta[#1], **Dipmoy Nath**[#1], **Yue Yang**[1], **Bao T. Le**[1], **Golam Mohi**[1,2]

[1]Department of Biochemistry and Molecular Genetics, University of Virginia School of Medicine, Charlottesville, VA 22908, USA

[2]University of Virginia Cancer Center, Charlottesville, VA 22908, USA

[#] These authors contributed equally to this work.

Abstract

Myelofibrosis (MF) is a deadly blood neoplasia with the worst prognosis among myeloproliferative neoplasms (MPN). The JAK2 inhibitors Ruxolitinib and Fedratinib have been approved for treatment of MF, but they do not offer significant improvement of bone marrow fibrosis. CDK6 expression is significantly elevated in MPN/MF hematopoietic progenitor cells. In this study, we investigated the efficacy of CDK4/6 inhibitor Palbociclib alone or in combination with Ruxolitinib in Jak2V617F and MPLW515L murine models of MF. Treatment with Palbociclib alone significantly reduced leukocytosis and splenomegaly and inhibited bone marrow fibrosis in Jak2V617F and MPLW515L mouse models of MF. Combined treatment of Palbociclib and Ruxolitinib resulted in normalization of peripheral blood leukocyte counts, marked reduction of spleen size, and abrogation of bone marrow fibrosis in murine models of MF. Palbociclib treatment also preferentially inhibited Jak2V617F mutant hematopoietic progenitors in mice. Mechanistically, treatment with Palbociclib or depletion of CDK6 inhibited Aurora kinase, NF-κB, and TGF-β signaling pathways in Jak2V617F mutant hematopoietic cells and attenuated expression of fibrotic markers in the bone marrow. Overall, these data suggest that Palbociclib in combination with Ruxolitinib may have therapeutic potential for treatment of MF and support the clinical investigation of this drug combination in patients with MF.

Keywords

Myelofibrosis; CDK6; JAK2; Palbociclib; Ruxolitinib

Introduction

Myelofibrosis (MF) is the most aggressive form of myeloproliferative neoplasms (MPN), characterized by bone marrow fibrosis, leukocytosis and extramedullary hematopoiesis. MF patients with intermediate and high-risk disease have a median survival of 16 to 35 months

Correspondence: Golam Mohi, Ph.D., Department of Biochemistry and Molecular Genetics, University of Virginia School of Medicine, Pinn Hall 6023, Charlottesville, VA 22908, Phone: 434-924-5657; Fax: 434-924-5069; gm7sj@virginia.edu.

Authorship

Contribution: A.D. performed research, analyzed data and wrote the manuscript; D.N. performed research and analyzed data, Y.Y performed research; B.T.L. performed data analysis; G.M. designed the research, analyzed data, and wrote the manuscript.

Conflicts of interest disclosure: The authors declare no potential conflicts of interest.

(1). The oncogenic JAK2V617F mutation was detected in 50–60% patients with MF (2, 3). Additional mutations in the thrombopoietin receptor (MPL) and calreticulin (CALR) were observed in MF (4–7). JAK2, MPL and CALR mutations are considered as MPN driver mutations and they lead to hyperactivation of the JAK/STAT signaling (3). The JAK1/2 inhibitor Ruxolitinib is approved for treatment of MF (8, 9). Although Ruxolitinib treatment provides symptomatic relief, it does not cure or significantly improve bone marrow (BM) fibrosis in patients with MF (10, 11) Moreover, initial responses to Ruxolitinib therapy are lost after prolonged treatment in many cases (12). Fedratinib, a new JAK2-selective inhibitor, has recently been approved for treatment of MF (13, 14). Fedratinib therapy also reduces splenomegaly and constitutional symptoms but does not significantly improve BM fibrosis. Thus, there is a critical need to develop novel therapies for MF that can effectively treat bone marrow fibrosis.

Cyclin-dependent kinase 6 (CDK6) and its close homolog CDK4 are known to regulate G1 to S phase cell cycle progression via activation of the CDK4/6-cyclin D complex and subsequent phosphorylation of the retinoblastoma (Rb) protein, which drives E2F-dependent transcription (15, 16). Mice deficient in Cdk6 are viable and they exhibit only minor defects in erythrocyte and thymocyte development (17, 18). Expression of CDK6 is upregulated in various hematologic malignancies (16). CDK6 is required for leukemogenesis mediated by MLL- and NUP98-fusion oncoproteins (19, 20). CDK6 can also act as a transcriptional regulator (16). Both kinase-independent and kinase-dependent functions for CDK6 have been suggested (21). CDK6 has been shown to interact with NF-kB subunit p65 and serve as a transcriptional coregulator of NF-kB-dependent gene expression (22). Inhibitors targeting CDK4/6 have been developed and undergoing testing in various human cancers (23). Three CDK4/6 inhibitors, Palbociclib, Ribociclib and Abemaciclib, have been approved for treatment of hormone receptor (HR)-positive advanced breast cancer.

We have found that expression of CDK6 is significantly elevated in hematopoietic progenitors of Jak2V617F knock-in mice and MF patients. In this study, we investigated the efficacy of CDK4/6 inhibitor Palbociclib alone and in combination with Ruxolitinib in Jak2V617F and MPLW515L murine models of MF. We show that Palbociclib in combination with Ruxolitinib normalizes blood leukocyte counts, reduces splenomegaly and remarkably improves BM fibrosis in both Jak2V617F and MPLW515L mouse models of MF.

Materials and Methods

Mice

Conditional Jak2V617F knock-in (24) and Mx1Cre (25) mice were previously described. Cre expression was induced by intraperitoneal injection of polyinosine-polycytosine (pI-pC) at 4 weeks after birth. To generate MPLW515L mouse model, 5-fluorouracil-primed BALB/c mice BM cells were transduced with MSCV-MPLW515L-IRES-GFP retroviruses and injected into lethally irradiated BALB/c (Jackson Laboratories; stock # 000651) recipient mice. For competitive BM reconstitution assay, BM cells from Mx1Cre; $Jak2^{VF/VF}$; GFP and wild type C57BL/6 mice (Jackson Laboratories; stock # 000664) were mixed at 1:1 ratio and injected into lethally irradiated C57BL/6 recipient mice. All animal

studies were performed in accordance with the guidelines approved by the IACUC of University of Virginia School of Medicine.

Patient samples

Peripheral blood and bone marrow samples from MF patients were collected at University of Virginia Cancer Center. Informed written consent from the subjects was obtained for sample collection according to the protocols approved by the institutional review board of the University of Virginia Health System and in accordance with the Declaration of Helsinki. Only adult patient samples were collected.

Cell cultures

Human HEL and SET-2 sells were from DSMZ. UKE-1 cell line was kindly provided by Dr. Ross Levine (MSKCC). Mouse parental BA/F3 cell line was obtained from Dr. James Griffin's Lab (Dana-Farber Cancer Institute). These cell lines were obtained between 2006 and 2011. BA/F3-EpoR-JAK2V617F, BA/F3-MPLW515L and BA/F3-MPL-CALR del52 cells were generated by Mohi lab and the cells were authenticated using PCR method. BA/F3-EpoR-JAK2V617F, BA/F3-MPLW515L and BA/F3-MPL-CALR del52 cells and human HEL and SET-2 cells were maintained in RPMI-1640 medium supplemented with 10% FBS and penicillin/streptomycin. UKE-1 cells were maintained in IMDM medium supplemented with 10% FBS, 10% DHS, 1 μM Hydrocortisone and penicillin/streptomycin. Cells were monitored under microscope for contamination. However, they were not tested for Mycoplasma. Cells were cultured for less than one month before use.

Inhibitors

Palbociclib and Ruxolitinib were purchased from Chemietek. To assess the in vivo efficacy of Palbociclib/Ruxolitinib in Jak2V617F model of MF, BM cells from Mx1Cre; $Jak2^{VF/VF}$ mice were transplanted into lethally irradiated C57BL/6 recipient mice. Six weeks after transplantation, mice were randomized to receive treatment with vehicle, Palbociclib (50mg/kg), Ruxolitinib (60mg/kg) or Palbociclib (50mg/kg) plus Ruxolitinib (60mg/kg) by oral gavage once daily for 6 weeks. MPLW515L BMT mice were treated with the drugs for 3 weeks.

Immunoblotting

SET-2 and HEL cells were washed in PBS following treatment with the inhibitors and lysed in RIPA lysis buffer containing protease inhibitors. Jak2V617F mouse BM cells and MF BM and PBMC were lysed directly by boiling in 2x sample buffer. Immunoblotting was performed using indicated phospho-specific or total antibodies. The following antibodies were used. Cell Signaling Technology: p-STAT5 (Tyr694) (#4322), STAT5 (#94205), p-RB (Ser795) (#9301), p-p65 (Ser536) (#3033), p-SMAD2 (Ser465/Ser467) (#18338), SMAD2 (#5339), Santa Cruz Biotechnology: p65 (#sc-372), CDK6 (#sc-177), RB (#sc-50). Sigma: β-Actin (#A5441), Abcam: HMGA2 (#ab202387), Abclonal: AURKA (#A2121), BD Biosciences: AURKB (#611082).

Immunostaining

Immunostaining for SNAIL and αSMA were performed as described below. Paraffin sections of BM were treated with 100% xylene for 5min twice, 100% xylene and 100/% ethanol 1:1 ratio for 3 min, 100% ethanol for 5 min twice, 95% ethanol for 5min, 70% ethanol for 5min and 50% ethanol for 5 min and rinsed with cold water for 1 min followed by antigen retrieval with sodium citrate buffer at 100°C for 20 min. Blocking was performed with 10% goat serum for 2 hours. Anti-SNAIL (Rabbit, 1:100, Abclonal), anti-αSMA (rabbit, 1:300, Abclonal) and were used for staining. Secondary staining was done using TRITC goat anti-rabbit antibody (1:200 dilution) (Jackson Immunoresearch) and mounted in vectashield mounting medium with DAPI (H-1200, Vector Labs). Fluorescence was visualized using Zeiss LAM 710 confocal microscope. Data were analyzed using Image J software (Image J). Scale bars, 15μm.

MSC culture and immunofluorescence staining

Mesenchymal stromal cells (MSC) were generated from mice BM as previously described (26). For immunofluorescence staining, MSCs were grown on cover slips and incubated with TGF-β1 (50ng/ml) for 72 hours in the presence or absence of Palbociclib (0.25μM). Collagen staining was performed with un-conjugated antibodies against Collagen I or Collagen III (Abcam). Secondary staining was done using TRITC goat anti-rabbit antibody (Jackson Immunoresearch). Fluorescence was visualized using Zeiss LAM 710 Confocal microscope.

RNA-sequencing

LSK ($Lin^{-}Sca1^{+}c\text{-}kit^{+}$) cells were sorted from $Jak2^{VF/VF}$ mice treated with vehicle, Palbociclib, Ruxolitinib or Palbociclib plus Ruxolitinib combination using a FACS Aria II (BD Biosciences). Total RNA was extracted from LSK cells using RNeasy Mini kit (Qiagen). RNA sequencing was performed using NEBNext Ultra II Directional RNA Library Prep Kit for Illumina (NEB) and Hiseq next-generation sequencing instrument (Illumina). Jak2V617F LT-HSC microarray data accession number: GSE79198. MPN patient data accession number: GSE54644. RNA-seq data generated in this study are deposited to NCBI GEO database (GSE173814).

Real-time quantitative PCR

Total RNA was extracted from LSK, MSC or SET-2 cells with RNeasy Mini kit (Qiagen) and cDNA samples were prepared by using QuantiTect Reverse Transcription kit (Qiagen). Real-time quantitative PCR (RT-qPCR) was performed in a Quantstudio3 machine (Applied Biosystems) using SYBR Green PCR master mix (Quatabio). The data were normalized to *GAPDH*, *18S* or *HPRT* and fold changes in gene expression were determined by the ΔΔCt method. Sequences of the primers are available in the Supplementary Tables 1 and 2.

Statistical analysis

Results are expressed as mean ± SEM, and statistical significance was determined by one-way analysis of variance (ANOVA) or Student's t-test using Prism Version 8 software (GraphPad, Prism). $P<0.05$ was considered statistically significant.

Results

CDK6 expression is significantly upregulated in MF

Using unbiased microarray gene expression analysis (GSE79198), we identified CDK6 as one of the significantly upregulated genes in long term hematopoietic stem cells (LT-HSC) of Jak2V617F knock-in mice (24) compared with control LT-HSC (Fig. 1A). Real-time quantitative PCR (RT-qPCR) further validated significantly increased expression of CDK6 in Jak2V617F LT-HSC as compared to wild-type LT-HSC (Fig. 1B). Analysis of MPN gene expression data set (GSE54644) revealed that CDK6 expression is significantly increased in MF patient's granulocytes compared with healthy controls (Fig. 1C). RT-qPCR further validated significantly elevated CDK6 mRNA expression in MF CD34+ cells compared with healthy control CD34+ cells (Fig. 1D).

Consistent with increased CDK6 mRNA expression, we observed elevated CDK6 protein levels in the bone marrow (BM) and peripheral blood mononuclear cells (PBMC) of MF patients compared with healthy controls (Fig. 1E–F). We also observed elevated CDK6 protein levels in the BM of Jak2V617F mice (Fig. 1G) as well as in mice expressing MPLW515L (Fig. 1H). We next assessed the CDK6 protein levels in hematopoietic BA/F3 cells expressing MPN driver mutants JAK2V617F, MPLW515L and CALRdel52. We found increased CDK6 protein levels in BA/F3 cells expressing JAK2V617F, MPLW515L or CALRdel52 mutant compared with BA/F3 parent cells (Fig. 1I), suggesting that all three MPN driver mutants can induce CDK6 expression.

We tested whether inhibition of JAK2 can affect CDK6 expression. We observed dose-dependent reduction of STAT5 phosphorylation but no significant change in CDK6 expression by Ruxolitinib treatment in HEL and MF PBMC cells (Supplementary Fig. 1A–B). Similarly, in vivo treatment of Ruxolitinib almost completely inhibited STAT5 phosphorylation but did not significantly affect CDK6 level or Rb phosphorylation in the BM of Jak2V617F knock-in ($Jak2^{VF/VF}$) mice (Supplementary Fig. 1C and Fig. 6G) suggesting that Ruxolitinib treatment does not inhibit CDK6 in MPN cells.

We next investigated the effects of CDK6 depletion on JAK2V617F-expressing hematopoietic cells. We observed that lentiviral shRNA-mediated knockdown of CDK6 significantly inhibited the proliferation of JAK2V617F-expressing murine BA/F3-EpoR-JAK2V617F cells and human SET-2 and HEL cells but not WT JAK2-expressing BA/F3-EpoR cells (Supplementary Fig. 2A–D). These suggest that CDK6 may play an important role in the growth/survival of MPN cells expressing oncogenic JAK2V617F mutant.

CDK6 inhibitor Palbociclib alone or in combination with Ruxolitinib significantly inhibits hematopoietic cells expressing MPN driver mutants

We investigated the effects of CDK6 inhibition by Palbociclib on proliferation of hematopoietic cells expressing JAK2V617F and MPLW515L. We found that Palbociclib treatment significantly reduced proliferation of murine BA/F3-EpoR-JAK2V617F and BAF3-MPLW515L cells whereas WT JAK2-expressing BA/F3 cells were modestly affected by Palbociclib treatment only at higher concentration (Fig. 2A–C). Palbociclib treatment also significantly inhibited proliferation of human JAK2V617F-positive HEL, SET-2 and

UKE-1 cells (Fig. 2D–F). Combined treatment of Palbociclib and Ruxolitinib resulted in greater inhibition of growth in BA/F3-EpoR-JAK2V617F, HEL and SET-2 cells (Fig. 2G–I). We also tested the effects Palbociclib or Palbociclib/Ruxolitinib combination on apoptosis in BA/F3-EpoR-JAK2V617F cells. Treatment of Palbociclib induced apoptosis in BA/F3-EpoR-JAK2V617F cells (Supplementary Fig. 3). Combined treatment of Palbociclib and Ruxolitinib caused marked increase in apoptosis of BA/F3-EpoR-JAK2V617F cells (Fig. 2J).

We also investigated the effects of Palbociclib/Ruxolitinib treatment on MF hematopoietic progenitors. CD34+ cells isolated from the peripheral blood of JAK2V617F-positive MF patients were plated in complete methylcellulose medium in the absence or presence of Palbociclib or Palbociclib/Ruxolitinib and hematopoietic progenitor colonies were assessed. Palbociclib alone significantly reduced myeloid colony formation in MF CD34+ progenitor cells (Fig. 2K). Combined treatment of Palbociclib with Ruxolitinib resulted in greater inhibition of colony formation in MF CD34+ cells (Fig. 2L). Palbociclib/Ruxolitinib treatment also caused reduction in myeloid colony formation in healthy control CD34+ cells (Supplementary Fig. 4A–B) although their effects were greater against MF CD34+ cells than healthy controls.

Treatment of Palbociclib alone or in combination with Ruxolitinib markedly inhibits myelofibrosis in Jak2V617F mouse model of MF

We previously reported the conditional Jak2V617F knock-in mice (24). Mice expressing homozygous Jak2V617F rapidly develop high-grade MF (24, 27). So, we utilized the homozygous Jak2V617F knock-in mice in this study to test the in vivo efficacy of Palbociclib alone or in combination with Ruxolitinib. BM cells from the homozygous Jak2V617F knock-in mice (Mx1Cre; $Jak2^{VF/VF}$) at 7 weeks after pI-pC induction were transplanted into lethally irradiated C57BL/6 recipient mice to generate a cohort of mice expressing $Jak2^{VF/VF}$. The experimental approach is depicted in Fig. 3A. At six weeks after BMT, all mice showed elevated WBC and neutrophil counts (Fig. 3B), indicating MPN disease development in these animals. Mice were then randomized into four groups to receive treatment with vehicle, Palbociclib (50 mg/kg), Ruxolitinib (60 mg/kg) or Palbociclib (50 mg/kg) plus Ruxolitinib (60 mg/kg) by oral gavage once daily for a period of 6 weeks. Treatment of Palbociclib alone significantly reduced WBC and neutrophil counts compared to vehicle treatment (Fig. 3B). Combined treatment of Palbociclib and Ruxolitinib normalized the WBC and neutrophil counts in these animals (Fig. 3B).

Flow cytometric analysis showed significant reduction in myeloid precursors ($Gr\text{-}1^+$/$Mac\text{-}1^+$) in the BM of $Jak2^{VF/VF}$ mice treated with Palbociclib or Palbociclib/Ruxolitinib combination (Fig. 3C). We also assessed the effects of Palbociclib/Ruxolitinib treatment on hematopoietic stem cells (HSC) and progenitors. We observed a significant reduction in LSK ($Lin^-Sca1^+c\text{-}Kit^+$), short-term HSC (ST-HSC), multipotent progenitors (MPP) in the BM of mice treated with Palbociclib/Ruxolitinib combination compared with vehicle treatment (Fig. 3D). In addition, we observed significant reduction of common myeloid progenitors (CMP), granulocyte-macrophage progenitors (GMP) and megakaryocyte-erythrocyte progenitors (MEP) in the BM of mice treated with Palbociclib/Ruxolitinib

combination compared with vehicle treatment (Fig. 3E). Hematopoietic progenitor colony assays showed significant reduction of CFU-GM colonies in the BM of Jak2$^{VF/VF}$ mice treated with Palbociclib or Palbociclib/Ruxolitinib combination compared with vehicle or Ruxolitinib treatment (Fig. 3F). Spleen size/weight was significantly reduced in Jak2$^{VF/VF}$ mice upon Palbociclib or Ruxolitinib treatment alone (Fig. 3G). Combined treatment of Palbociclib and Ruxolitinib resulted in significantly greater reduction of spleen size/weight in Jak2$^{VF/VF}$ mice (Fig. 3G).

Histopathologic analyzes revealed extensive BM fibrosis in vehicle-treated Jak2$^{VF/VF}$ mice (Fig. 3H). Palbociclib treatment alone caused marked reduction of fibrosis in the BM of Jak2$^{VF/VF}$ mice whereas Ruxolitinib treatment did not significantly alter BM fibrosis (Fig. 3H). Combined treatment of Palbociclib and Ruxolitinib almost completely ablated fibrosis in the BM of Jak2$^{VF/VF}$ mice (Fig. 3H).

Palbociclib treatment preferentially inhibits Jak2V617F mutant hematopoietic progenitors

To evaluate whether Palbociclib can effectively inhibit disease causing Jak2V617F mutant stem/progenitor cells, we generated Mx1Cre; Jak2$^{VF/VF}$ GFP+ mice and performed competitive BM transplantation assays followed by drug treatments. BM cells from Mx1Cre; Jak2$^{VF/VF}$ GFP+ mice (6 weeks after pI-pC induction) were mixed with WT C57BL/6 mice BM cells at a ratio of 1:1 and then transplanted into lethally irradiated C57BL/6 mice (outlined in Fig. 4A). At 6 weeks after BMT, mice were randomized to receive treatment with vehicle, Palbociclib (50 mg/kg), Ruxolitinib (60 mg/kg) or Palbociclib (50 mg/kg) plus Ruxolitinib (60 mg/kg) by oral gavage once daily for a period of 12 weeks. Treatment of Palbociclib alone significantly reduced the WBC and neutrophil counts compared with vehicle treatment (Fig. 4B). Combined treatment of Palbociclib and Ruxolitinib resulted in normalization of WBC and neutrophil counts (Fig. 4B). Vehicle-treated chimeric mice exhibited high percentage (60–70%) of GFP+ LSK and LK (Lin^{-}c-Kit^{+}) cells in their BM (Fig. 4C–D). Treatment of Palbociclib or Palbociclib/Ruxolitinib combination significantly reduced the percentage of mutant GFP+ LSK and LK cells in the chimeric mice (Fig. 4C–D). Treatment of Palbociclib or Palbociclib/Ruxolitinib combination also caused significant reduction in the percentage of mutant GFP+ myeloid (Gr-1^{+}) and megakaryocytic (CD41^{+}) cells in the BM of chimeric mice (Fig. 4E–F). Together, these results suggest that Palbociclib treatment preferentially inhibits oncogenic Jak2V617F mutant hematopoietic progenitors.

To determine if the effects of Palbociclib or Palbociclib/Ruxolitinib treatment on mutant HSPC could sustain overtime after withdrawal of the treatment, we performed secondary transplantation experiment using BM from the primary transplanted chimeric mice after 12 weeks of treatment into lethally irradiated WT C57BL/6 recipient mice. The secondary transplanted mice were not given any treatment and they were analyzed at 16 weeks after transplantation (as outlined in Fig. 4G). We observed significantly reduced percentage of mutant GFP+ LSK and LK cells in the recipients of Palbociclib-treated mice BM compared with recipients of vehicle-treated mice BM (Fig. 4H–I). Recipients of BM from Jak2$^{VF/VF}$ GFP+ chimeric mice that were initially treated with Palbociclib/Ruxolitinib combination exhibited greater reduction of GFP+ LSK and LK cells compared with recipients of single

drug-treated mice BM (Fig. 4H–I). Recipients of Palbociclib- or Palbociclib/Ruxolitinib-treated mice BM also exhibited significant reduction in the percentage of mutant GFP+ myeloid (Gr-1$^+$) and megakaryocytic (CD41$^+$) cells compared with recipients of vehicle or Ruxolitinib-treated mice BM (Fig. 4J–K). Thus, decrease in mutant HSPC and myeloid/megakaryocytic precursors caused by the treatment of Palbociclib- or Palbociclib/Ruxolitinib was sustained overtime even after discontinuation of the treatment, i.e., withdrawal of Palbociclib or Palbociclib/Ruxolitinib combination treatment did not lead to recurrence of the disease in the secondary recipients.

Treatment of Palbociclib or Palbociclib/Ruxolitinib combination significantly inhibits myelofibrosis in MPLW515L mouse model of MF

We also tested the in vivo efficacy of Palbociclib and Palbociclib/Ruxolitinib combination in MPLW515L mouse model of MF (28). We generated a cohort of mice expressing MPLW515L by transduction of BALB/c mice BM cells with MSCV-MPLW515L retroviruses followed by transplantation into lethally irradiated syngeneic recipient mice. At three weeks after transplantation, mice were randomized to receive treatment with placebo (vehicle), Palbociclib (50 mg/kg), Ruxolitinib (60 mg/kg) or Palbociclib (50 mg/kg) plus Ruxolitinib (60 mg/kg) (outlined in Fig. 5A). Whereas vehicle-treated MPLW515L mice exhibited markedly increased WBC, neutrophil and platelet counts in their peripheral blood, Palbociclib-treated animals exhibited significant decrease in peripheral blood WBC, neutrophil and platelet counts (Fig. 5B). Ruxolitinib treatment also caused reduction in blood counts. However, combined treatment of Palbociclib and Ruxolitinib resulted in almost complete normalization of WBC, neutrophil and platelet counts in these animals (Fig. 5B). Flow cytometric analysis revealed that Palbociclib or Palbociclib/Ruxolitinib combination treatment significantly reduced myeloid precursors (Gr-1$^+$/Mac-1$^+$) and megakaryocytic precursors (CD61$^+$/CD41$^+$) in the BM and spleens of MPLW515L mice (Fig. 5C–F). Marked splenomegaly was observed in vehicle-treated MPLW515L mice (Fig. 5G). Palbociclib treatment alone significantly reduced splenomegaly in MPLW515L mice (Fig. 5G). However, combined treatment of Palbociclib and Ruxolitinib resulted in greater reduction of spleen size/weight than single drug treatment (Fig. 5G). Histopathologic analyzes showed that Palbociclib treatment alone caused marked reduction of BM fibrosis whereas Ruxolitinib treatment did not exhibit significant reduction of BM fibrosis in MPLW515L mice (Fig. 5H). Combined treatment of Palbociclib with Ruxolitinib ablated BM fibrosis in MPLW515L mice (Fig. 5H). Together, these data suggest that Palbociclib treatment alone or in combination with Ruxolitinib might be efficacious in the treatment of MF.

Inhibition of CDK6 by Palbociclib alters gene expression and impairs cell signaling in hematopoietic progenitors expressing Jak2V617F

To gain insights into the mechanisms by which CDK6 inhibition ameliorates myelofibrosis, we performed RNA-sequencing on LSK cells from Jak2$^{VF/VF}$ mice treated with the inhibitors. Heat map showed significantly down-regulated genes in Palbociclib- and Palbociclib/Ruxolitinib-treated LSK cells compared with vehicle-treated LSK cells (Fig. 6A). Gene Set Enrichment Analysis (GSEA)(29) of RNA-sequencing data revealed significant down regulation of genes related to cell cycle, stem cells, Aurora kinase

(AURK) and NF-κB signaling pathways in Palbociclib-treated LSK cells compared with vehicle-treated LSK cells (Fig. 6B). These pathways were also similarly affected in Palbociclib/Ruxolitinib-treated mice LSK cells compared to Ruxolitinib-treated LSK cells (Supplementary Fig. 5A).

We next compared genes that were significantly downregulated by Palbociclib treatment with genes that were upregulated in MF gene expression dataset (GSE54644). There was an overlap of 245 genes, which were upregulated in MF patients and significantly downregulated in Palbociclib-treated Jak2$^{VF/VF}$ mice LSK cells (Fig. 6C). Molecular signature analysis of overlapping genes showed enrichment for cell cycle, Rb1 targets, cell proliferation, inflammatory response and Aurora kinase pathway (Fig. 6C), indicating that these pathways were upregulated in MF and downregulated by Palbociclib treatment.

RNA-seq data analysis revealed that expression of AURKA, AURKB and HMGA2 was significantly reduced in Palbociclib-treated Jak2$^{VF/VF}$ mice LSK cells compared with vehicle-treated Jak2$^{VF/VF}$ mice LSK cells. RT-qPCR further validated that expression of AURKA, AURKB and HMGA2 was significantly downregulated in Palbociclib- and Palbociclib/Ruxolitinib-treated LSK cells compared with vehicle-treated LSK cells (Fig. 6D). Interestingly, expression of AURKA, AURKB and HMGA2 is significantly elevated in MF patient's hematopoietic cells as compared to healthy controls (Supplementary Fig. 5B). Lentiviral shRNA-mediated knockdown of CDK6 also significantly reduced the expression of AURKA, AURKB and HMGA2 in SET-2 cells (Fig. 6E) similar to that observed with Palbociclib treatment (Supplementary Fig. 5C) suggesting that they are bona fide targets of CDK6.

We next performed cell signaling studies in MF patient PBMC and Jak2$^{VF/VF}$ mice BM following treatment with Palbociclib or Palbociclib/Ruxolitinib combination. As expected, we observed decreased Rb phosphorylation upon Palbociclib treatment in MF PBMC and Jak2$^{VF/VF}$ BM cells (Fig. 6F–G). Ruxolitinib treatment, however, did not cause significant inhibition of Rb phosphorylation in these cells (Fig. 6F–G). We also observed reduced expression of HMGA2, AURKA and AURKB proteins in MF PBMC and Jak2$^{VF/VF}$ BM cells upon Palbociclib or Palbociclib/Ruxolitinib treatment (Fig. 6F–G). Since CDK6 has been shown to regulate the NF-κB signaling pathway (22), we also assessed the effects of Palbociclib on NF-κB signaling. Indeed, we observed reduced p65 phosphorylation in MF PBMC and Jak2$^{VF/VF}$ mice BM treated with Palbociclib or Palbociclib/Ruxolitinib (Fig. 6F–G). To further confirm that the signaling alterations caused by Palbociclib treatment in MF PBMC and Jak2$^{VF/VF}$ mice BM was due to inhibition of CDK6, we performed shRNA-mediated knockdown of CDK6 in SET-2 cells. We observed marked inhibition of Rb and p65 phosphorylation and decreased expression of HMGA2, AURKA and AURKB proteins upon CDK6 knockdown in SET-2 cells (Fig. 6H) similar to that observed with Palbociclib treatment (Supplementary Fig. 6).

Palbociclib treatment reduces the TGF-β1 level and attenuates expression of fibrotic markers

Analysis of the RNA-seq data also revealed that genes related to TGF-β signaling was significantly downregulated in Palbociclib-treated Jak2$^{VF/VF}$ mice LSK cells (Fig. 7A). We

showed previously that HMGA2 regulates TGF-β1 expression (26). Furthermore, increased levels of TGF-β1 have been found in patients with MF (30), and TGF-β1 has been suggested to play a role in the pathogenesis of MF (31, 32). We observed that Palbociclib treatment significantly reduced serum TGF-β1 level in $Jak2^{VF/VF}$ mice (Fig. 7B). We also observed a marked decrease in SMAD2 phosphorylation, a downstream target of the TGF-β signaling, in MF PBMC, $Jak2^{VF/VF}$ mice BM and SET-2 cells upon Palbociclib treatment (Fig. 7C–E). Combined treatment of Palbociclib and Ruxolitinib resulted in greater inhibition of SMAD2 phosphorylation in MF PBMC and $Jak2^{VF/VF}$ mice BM (Fig. 7C–D). Knockdown of CDK6 also resulted in similar decrease in SMAD2 phosphorylation in SET-2 cells (Fig. 7F). Thus, suppression of CDK6 activity by gene depletion or Palbociclib treatment can downmodulate the TGF-β signaling pathway. In addition, we observed that in vivo treatment of Palbociclib alone or in combination with Ruxolitinib significantly reduced serum levels of IL-6 and IL-1β in $Jak2^{VF/VF}$ mice (Supplementary Fig. 7A and B), suggesting that Palbociclib/Ruxolitinib combination treatment can alleviate inflammation.

Next, we assessed the levels of fibrotic markers in the BM following Palbociclib treatment. Collagen deposition in the BM stromal cells is directly linked to myelofibrosis (30). We previously showed that TGF-β1 stimulation significantly increased Collagen I and III expression in the BM mesenchymal stromal cells (MSC) (26). Since we observed that Palbociclib treatment inhibits the TGF-β signaling pathway, we asked if Palbociclib treatment could inhibit TGF-β1-induced Collagen expression in BM MSC. Indeed, we observed that Palbociclib significantly inhibited TGF-β1-induced Collagen I and III expression in BM MSC (Fig. 7G). Ruxolitinib treatment, however, did not significantly inhibit TGF-β1-induced Collagen I and III expression in BM MSC (Supplementary Fig. 8). Immunofluorescence staining also showed that Palbociclib treatment markedly reduced TGF-β1-induced Collagen I and III expression in the BM MSC (Fig. 7H).

TGF-β1 can also induce Snail and α-smooth muscle actin (αSMA), which promote epithelial-mesenchymal transition (EMT) and extracellular matrix (ECM) production in different types of tissue fibrosis and cancer (33, 34). We found that expression of Snail and αSMA was significantly elevated upon TGF-β1 stimulation, and treatment of Palbociclib almost completely inhibited TGF-β1-induced Snail and αSMA expression in the BM MSC (Fig. 7I). Immunohistochemistry analysis on the BM sections from vehicle-treated $Jak2^{VF/VF}$ mice showed high level expression of Snail and αSMA (Fig. 7J). Palbociclib treatment alone or in combination with Ruxolitinib significantly reduced Snail and αSMA expression whereas Ruxolitinib treatment alone had little or no effect on their expression (Fig. 7J). These data strongly suggest that inhibition of CDK6 by Palbociclib blocks TGF-β1-induced upregulation of fibrotic factors in the BM and thus prevent the development and progression of myelofibrosis.

Discussion

Myelofibrosis is the most severe form of MPN with limited treatment options. Currently approved JAK2 inhibitors provide only symptomatic relief without offering significant reduction in bone marrow fibrosis (12). Complete remissions similar to those observed in CML with ABL kinase inhibitors cannot be achieved with current JAK2 inhibitors in

MF. So, there is an unmet critical need for development of new therapeutic approaches for treatment of MF.

CDK6 is known to regulate G1 to S phase transition of the cell cycle (15, 16). However, CDK6 is not essential for mammalian cell cycle (15,17) and hematopoiesis appears to be normal in CDK6-deficient mice under steady-state conditions (35). Dysregulated expression of CDK6 has been observed in a variety of malignancies (16). It has been shown recently that loss of CDK6 attenuates the development of PV-like MPN in mice although CDK6 inhibition by Palbociclib does not significantly improve PV disease in $Jak2^{V617F/+}$ mice (36). The contribution of CDK6 in MF pathogenesis and the effects of CDK6 inhibition against MF has remained unknown.

We found significant upregulation of CDK6 expression in hematopoietic progenitors of Jak2V617F knock-in mice and MF patients. So, we evaluated the efficacy of CDK4/6 inhibitor Palbociclib alone or in combination with JAK1/2 inhibitor Ruxolitinib in hematopoietic cells expressing MPN driver mutants and murine models of MF. We tested Palbociclib since it is a well-tolerated FDA-approved drug for treatment of HR-positive advanced breast cancer (37). We demonstrate that Palbociclib treatment significantly inhibits the growth/survival of hematopoietic cells expressing JAK2V617F and MPLW515L. Palbociclib treatment also caused pronounced inhibition of clonogenic growth of MF patient CD34+ cells. More importantly, Palbociclib treatment alone markedly reduced splenomegaly and BM fibrosis in $Jak2^{VF/VF}$ and MPLW515L mouse models of MF. The effects of Palbociclib in reducing splenomegaly and BM fibrosis were even more pronounced than those observed with currently approved Ruxolitinib therapy. Combined treatment of Palbociclib/Ruxolitinib resulted in almost complete inhibition of BM fibrosis in $Jak2^{VF/VF}$ and MPLW515L mouse models. Thus, our data suggest that Palbociclib alone or in combination with Ruxolitinib may have therapeutic potential for treatment of MF.

Previous studies have suggested that CDK6 can act as a transcriptional regulator (16, 21, 22). Using transcriptome analysis, we found that expression of AURKA, AURKB and HMGA2 was significantly downregulated in $Jak2^{VF/VF}$ LSK by Palbociclib or Palbociclib/Ruxolitinib treatment. AURKA and AURKB play an important role in cell cycle progression during mitosis and cytokinesis, and their aberrant expression has been associated with various malignancies (38, 39). Previous studies also have shown that inhibition of AURKA/AURKB can reduce the growth and survival of JAK2V617F-positive MPN cells and attenuate the BM fibrosis in mouse models of MPN (40, 41). HMGA2 is a chromatin-binding protein that plays a role in the self-renewal of HSC (42). Overexpression of HMGA2 has been observed in MF progenitors (43, 44). We showed previously that HMGA2 regulates TGF-β1 expression and promotes the development of MF in Jak2V617F mice (26). Since Palbociclib can inhibit both CDK4 and CDK6, we performed CDK6 knockdown in JAK2V617F-positive SET-2 cells. We observed that knockdown of CDK6 significantly reduced expression of AURKA, AURKB and HMGA2 similar to that observed with Palbociclib treatment. Therefore, AURKA, AURKB and HMGA2 are bona fide targets of CDK6, and inhibition of CDK6 by Palbociclib may inhibit the MPN cells and ameliorates myelofibrosis by downregulation of these target genes. Future studies will determine how inhibition of CDK6 by Palbociclib regulates the expression of these genes.

We observed downregulation of NF-κB pathway in Jak2$^{VF/VF}$ LSK cells and reduced phosphorylation of NF-κB p65 subunit in MF primary cells and Jak2$^{VF/VF}$ mice BM by Palbociclib treatment. NF-κB is known as a master regulator of inflammation, and constitutive activation of NF-κB has been observed in MPN/MF (45). It has been shown that CDK6 interacts with p65 and regulates the expression of NF-κB target genes (22). A recent study also suggested that CDK6-deficiency downregulates the expression of NF-κB target genes in Jak2V617F mouse LSK cells (36). We also observed significant reduction of IL-6 and IL-1β levels in Jak2$^{VF/VF}$ mice treated with Palbociclib/Ruxolitinib combination. Thus, combined treatment of Palbociclib and Ruxolitinib might attenuate the MF phenotype by inhibiting the inflammatory pathway.

Previous reports have suggested an important role for TGF-β signaling in various tissue fibrosis (33, 46). Increased levels of TGF-β1 also have been observed in patients with MF as well as in mouse models of MF (30–32, 47). We observed downregulation of genes related to TGF-β signaling in Palbociclib-treated Jak2$^{VF/VF}$ mice LSK cells. We also observed decreased serum levels of TGF-β1 in Jak2$^{VF/VF}$ mice treated with Palbociclib. In addition, we observed decreased phosphorylation of SMAD2 following treatment with Palbociclib as well as with knockdown of CDK6. TGF-β1 can induce the expression of Collagen, Snail and αSMA, which have been implicated in tissue fibrosis and cancer metastasis (34, 48). Palbociclib treatment significantly reduced the TGF-β1 induced Collagen (I and III), Snail and αSMA expression in BM MSC. We also observed that treatment of Palbociclib significantly reduced Snail and αSMA expression in the BM of Jak2$^{VF/VF}$ mice. Thus, Palbociclib treatment may prevent the development/progression of BM fibrosis by inhibiting the TGF-β signaling and reducing the expression of fibrotic markers.

In summary, we demonstrate that inhibition of CDK6 by Palbociclib significantly inhibits MPN cells and progenitors and ameliorates BM fibrosis in multiple murine models of MF. Palbociclib treatment preferentially inhibits the mutant hematopoietic progenitors. We also show that dual targeting of CDK6 and JAK2 using Palbociclib and Ruxolitinib provides greater inhibition of MPN cells and more pronounced inhibition of BM fibrosis. Palbociclib treatment can induce myelosuppression in breast cancer patients. A combinatorial therapeutic approach involving Palbociclib and Ruxolitinib will enable lowering the doses of each of the inhibitors and thus reducing toxicities while enhancing the therapeutic efficacy. Results from our study support the clinical investigation of Palbociclib and Ruxolitinib combination in patients with MF.

Supplementary Material

Refer to Web version on PubMed Central for supplementary material.

Acknowledgements

We thank Matthew Stuver for assistance with CDK6 knockdown studies in cell lines. We also thank the Flow Cytometry and Microscopy Core Facilities and the Biorepository and Tissue Research Facility (BTRF) of the University of Virginia for assistance with FACS sorting, confocal microscopy and MPN specimen procurement and processing. Flow Cytometry and Microscopy Cores are supported by the UVA Cancer Center through P30CA044578 grant. This work was supported by grants from the National Institutes of Health (R01 HL095685, R01 HL149893, R21 CA235472) awarded to G.M.

References

1. Gangat N, Caramazza D, Vaidya R, George G, Begna K, Schwager S, et al.DIPSS plus: a refined Dynamic International Prognostic Scoring System for primary myelofibrosis that incorporates prognostic information from karyotype, platelet count, and transfusion status. J Clin Oncol2011;29:392–7 [PubMed: 21149668]
2. Levine RL, Gilliland DG. Myeloproliferative disorders. Blood2008;112:2190–8 [PubMed: 18779404]
3. Vainchenker W, Kralovics R. Genetic basis and molecular pathophysiology of classical myeloproliferative neoplasms. Blood2017;129:667–79 [PubMed: 28028029]
4. Pikman Y, Lee BH, Mercher T, McDowell E, Ebert BL, Gozo M, et al.MPLW515L is a novel somatic activating mutation in myelofibrosis with myeloid metaplasia. PLoS Med2006;3:e270 [PubMed: 16834459]
5. Pardanani AD, Levine RL, Lasho T, Pikman Y, Mesa RA, Wadleigh M, et al.MPL515 mutations in myeloproliferative and other myeloid disorders: a study of 1182 patients. Blood2006;108:3472–6 [PubMed: 16868251]
6. Nangalia J, Massie CE, Baxter EJ, Nice FL, Gundem G, Wedge DC, et al.Somatic CALR mutations in myeloproliferative neoplasms with nonmutated JAK2. N Engl J Med2013;369:2391–405 [PubMed: 24325359]
7. Klampfl T, Gisslinger H, Harutyunyan AS, Nivarthi H, Rumi E, Milosevic JD, et al.Somatic mutations of calreticulin in myeloproliferative neoplasms. N Engl J Med2013;369:2379–90 [PubMed: 24325356]
8. Harrison C, Kiladjian JJ, Al-Ali HK, Gisslinger H, Waltzman R, Stalbovskaya V, et al.JAK inhibition with ruxolitinib versus best available therapy for myelofibrosis. N Engl J Med2012;366:787–98 [PubMed: 22375970]
9. Verstovsek S, Mesa RA, Gotlib J, Levy RS, Gupta V, DiPersio JF, et al.A double-blind, placebo-controlled trial of ruxolitinib for myelofibrosis. N Engl J Med2012;366:799–807 [PubMed: 22375971]
10. Mascarenhas J, Hoffman R. A comprehensive review and analysis of the effect of ruxolitinib therapy on the survival of patients with myelofibrosis. Blood2013;121:4832–7 [PubMed: 23570800]
11. Pardanani A, Tefferi A. Definition and management of ruxolitinib treatment failure in myelofibrosis. Blood Cancer J2014;4
12. Harrison CN, Schaap N, Mesa RA. Management of myelofibrosis after ruxolitinib failure. Ann Hematol2020;99:1177–91 [PubMed: 32198525]
13. Harrison CN, Schaap N, Vannucchi AM, Kiladjian JJ, Tiu RV, Zachee P, et al.Janus kinase-2 inhibitor fedratinib in patients with myelofibrosis previously treated with ruxolitinib (JAKARTA-2): a single-arm, open-label, non-randomised, phase 2, multicentre study. Lancet Haematol2017;4:e317–e24 [PubMed: 28602585]
14. Mullally A, Hood J, Harrison C, Mesa R. Fedratinib in myelofibrosis. Blood Adv2020;4:1792–800 [PubMed: 32343799]
15. Malumbres M, Barbacid M. Cell cycle, CDKs and cancer: a changing paradigm. Nat Rev Cancer2009;9:153–66 [PubMed: 19238148]
16. Tigan AS, Bellutti F, Kollmann K, Tebb G, Sexl V. CDK6-a review of the past and a glimpse into the future: from cell-cycle control to transcriptional regulation. Oncogene2016;35:3083–91 [PubMed: 26500059]
17. Malumbres M, Sotillo R, Santamaría D, Galán J, Cerezo A, Ortega S, et al.Mammalian cells cycle without the D-type cyclin-dependent kinases Cdk4 and Cdk6. Cell2004;118:493–504 [PubMed: 15315761]
18. Hu MG, Deshpande A, Enos M, Mao D, Hinds EA, Hu GF, et al.A requirement for cyclin-dependent kinase 6 in thymocyte development and tumorigenesis. Cancer Res2009;69:810–8 [PubMed: 19155308]
19. Placke T, Faber K, Nonami A, Putwain SL, Salih HR, Heidel FH, et al.Requirement for CDK6 in MLL-rearranged acute myeloid leukemia. Blood2014;124:13–23 [PubMed: 24764564]

20. Schmoellerl J, Barbosa IAM, Eder T, Brandstoetter T, Schmidt L, Maurer B, et al.CDK6 is an essential direct target of NUP98 fusion proteins in acute myeloid leukemia. Blood2020;136:387–400 [PubMed: 32344427]
21. Kollmann K, Heller G, Schneckenleithner C, Warsch W, Scheicher R, Ott RG, et al.A kinase-independent function of CDK6 links the cell cycle to tumor angiogenesis. Cancer Cell2013;24:167–81 [PubMed: 23948297]
22. Handschick K, Beuerlein K, Jurida L, Bartkuhn M, Müller H, Soelch J, et al.Cyclin-dependent kinase 6 is a chromatin-bound cofactor for NF-κB-dependent gene expression. Mol Cell2014;53:193–208 [PubMed: 24389100]
23. Asghar U, Witkiewicz AK, Turner NC, Knudsen ES. The history and future of targeting cyclin-dependent kinases in cancer therapy. Nat Rev Drug Discov2015;14:130–46 [PubMed: 25633797]
24. Akada H, Yan D, Zou H, Fiering S, Hutchison RE, Mohi MG. Conditional expression of heterozygous or homozygous Jak2V617F from its endogenous promoter induces a polycythemia vera-like disease. Blood2010;115:3589–97 [PubMed: 20197548]
25. Kühn R, Schwenk F, Aguet M, Rajewsky K. Inducible gene targeting in mice. Science1995;269:1427–9 [PubMed: 7660125]
26. Dutta A, Hutchison RE, Mohi G. Hmga2 promotes the development of myelofibrosis in Jak2 V617F knockin mice by enhancing TGF-β1 and Cxcl12 pathways. Blood2017;130:920–32 [PubMed: 28637665]
27. Akada H, Akada S, Hutchison RE, Mohi G. Loss of wild-type Jak2 allele enhances myeloid cell expansion and accelerates myelofibrosis in Jak2V617F knock-in mice. Leukemia2014;28:1627–35 [PubMed: 24480985]
28. Koppikar P, Abdel-Wahab O, Hedvat C, Marubayashi S, Patel J, Goel A, et al.Efficacy of the JAK2 inhibitor INCB16562 in a murine model of MPLW515L-induced thrombocytosis and myelofibrosis. Blood2010;115:2919–27 [PubMed: 20154217]
29. Subramanian A, Tamayo P, Mootha VK, Mukherjee S, Ebert BL, Gillette MA, et al.Proc Natl Acad Sci U S A2005;102:15545–50 [PubMed: 16199517]
30. Yue L, Bartenstein M, Zhao W, Ho WT, Han Y, Murdun C, et al.Efficacy of ALK5 inhibition in myelofibrosis. JCI Insight2017;2:e90932 [PubMed: 28405618]
31. Chagraoui H, Komura E, Tulliez M, Giraudier S, Vainchenker W, Wendling F. Prominent role of TGF-beta 1 in thrombopoietin-induced myelofibrosis in mice. Blood2002;100:3495–503 [PubMed: 12393681]
32. Zingariello M, Martelli F, Ciaffoni F, Masiello F, Ghinassi B, D'Amore E, et al.Characterization of the TGF-β1 signaling abnormalities in the Gata1low mouse model of myelofibrosis. Blood2013;121:3345–63 [PubMed: 23462118]
33. Frangogiannis NTransforming growth factor-β in tissue fibrosis. J Exp Med2020;217:e20190103. [PubMed: 32997468]
34. Su J, Morgani SM, David CJ, Wang Q, Er EE, Huang YH, et al.TGF-β orchestrates fibrogenic and developmental EMTs via the RAS effector RREB1. Nature2020;577:566–71 [PubMed: 31915377]
35. Scheicher R, Hoelbl-Kovacic A, Bellutti F, Tigan AS, Prchal-Murphy M, Heller G, et al.CDK6 as a key regulator of hematopoietic and leukemic stem cell activation. Blood2015;125:90–101 [PubMed: 25342715]
36. Uras IZ, Maurer B, Nivarthi H, Jodl P, Kollmann K, Prchal-Murphy M, et al.CDK6 coordinates JAK2 V617F mutant MPN via NF-κB and apoptotic networks. Blood2019;133:1677–90 [PubMed: 30635286]
37. Turner NC, Ro J, André F, Loi S, Verma S, Iwata H, et al.Palbociclib in Hormone-Receptor-Positive Advanced Breast Cancer. N Engl J Med2015;373:209–19 [PubMed: 26030518]
38. Willems E, Dedobbeleer M, Digregorio M, Lombard A, Lumapat PN, Rogister B. The functional diversity of Aurora kinases: a comprehensive review. Cell Div2018;13:7 [PubMed: 30250494]
39. Borisa AC, Bhatt HG. A comprehensive review on Aurora kinase: Small molecule inhibitors and clinical trial studies. Eur J Med Chem2017;140:1–19 [PubMed: 28918096]
40. Wen QJ, Yang Q, Goldenson B, Malinge S, Lasho T, Schneider RK, et al.Targeting megakaryocytic-induced fibrosis in myeloproliferative neoplasms by AURKA inhibition. Nat Med2015;21:1473–80 [PubMed: 26569382]

41. Lima K, Carlos JAEG, Alves-Paiva RM, Vicari HP, Souza Santos FP, Hamerschlak N, et al.Reversine exhibits antineoplastic activity in JAK2 V617F-positive myeloproliferative neoplasms. Sci Rep2019;9:9895 [PubMed: 31289316]

42. Copley MR, Babovic S, Benz C, Knapp DJ, Beer PA, Kent DG, et al.The Lin28b-let-7-Hmga2 axis determines the higher self-renewal potential of fetal haematopoietic stem cells. Nat Cell Biol2013;15:916–25 [PubMed: 23811688]

43. Guglielmelli P, Zini R, Bogani C, Salati S, Pancrazzi A, Bianchi E, et al.Molecular profiling of CD34+ cells in idiopathic myelofibrosis identifies a set of disease-associated genes and reveals the clinical significance of Wilms' tumor gene 1 (WT1). Stem Cells2007;25:165–73 [PubMed: 16990584]

44. Harada-Shirado K, Ikeda K, Ogawa K, Ohkawara H, Kimura H, Kai T, et al.Dysregulation of the MIRLET7/HMGA2 axis with methylation of the CDKN2A promoter in myeloproliferative neoplasms. Br J Haematol2015;168:338–49 [PubMed: 25236537]

45. Kleppe M, Koche R, Zou L, van Galen P, Hill CE, Dong L, et al.Dual Targeting of Oncogenic Activation and Inflammatory Signaling Increases Therapeutic Efficacy in Myeloproliferative Neoplasms. Cancer Cell2018;33:29–43 [PubMed: 29249691]

46. Henderson NC, Rieder F, Wynn TA. Fibrosis: from mechanisms to medicines. Nature2020;587:555–66 [PubMed: 33239795]

47. Tefferi APathogenesis of myelofibrosis with myeloid metaplasia. J Clin Oncol2005;23:8520–30 [PubMed: 16293880]

48. Batlle E, Massagué J. Transforming Growth Factor-β Signaling in Immunity and Cancer. Immunity2019;50:924–40 [PubMed: 30995507]

Significance

These findings demonstrate that CDK6 inhibitor Palbociclib in combination with Ruxolitinib ameliorates myelofibrosis, suggesting this drug combination could be an effective therapeutic strategy against this devastating blood disorder.

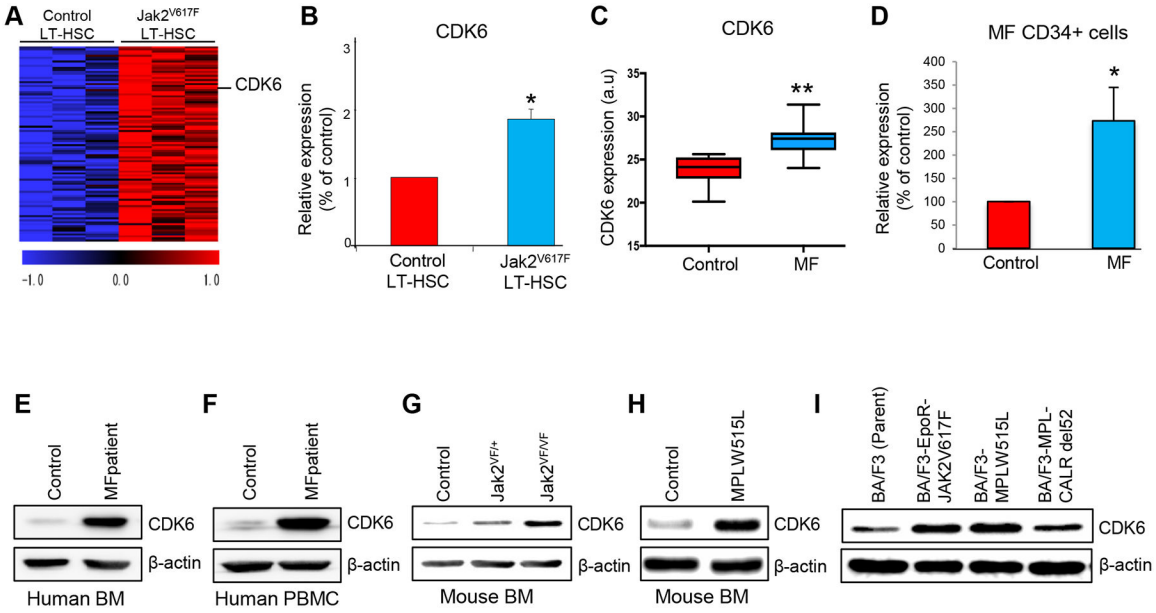

Figure 1. CDK6 expression is significantly increased in MF.

A, Heat map from microarray data analysis (GSE79198) showing significantly increased CDK6 expression in Jak2^{V617F} mice LT-HSC (Lin^{-}Sca-1^{+}c-kit^{+}CD34^{-}CD135^{-}) compared with control mice LT-HSC. **B,** RT-qPCR analysis shows significant increase of CDK6 mRNA expression in Jak2^{V617F} LT-HSC mice compared with control LT-HSC (n=4). The mRNA expression was normalized with *18S*. **C,** Analysis of MPN microarray gene expression data (GSE54644) shows that CDK6 expression is significantly increased in granulocytes of MF patients compared with healthy controls. (controls= 11, MF=18). **D,** RT-qPCR analysis shows significant increase of CDK6 mRNA expression in MF CD34+ cells compared with healthy control CD34+ cells (n=4). The mRNA expression was normalized with *18S* expression. **E** and **F,** Immunoblots showing elevated expression of CDK6 protein in the BM and PBMC of MF patients compared with healthy controls. β-actin served as a loading control. **G,** Increased CDK6 protein expression in the BM of Jak2V617F heterozygous (Jak2$^{VF/+}$) and homozygous (Jak2$^{VF/VF}$) mice compared with wild type control. Erk2 served as a loading control. **H,** Increased CDK6 protein expression in the BM of mice expressing MPLW515L compared with control mice. **I,** Elevated CDK6 protein expression in BA/F3-EpoR-JAK2V617F, BA/F3-MPLW515L and BA/F3-MPL-CALR del52 cells compared with parental BA/F3 cells. (* p<0.05; ** p<0.005; Student's t-test).

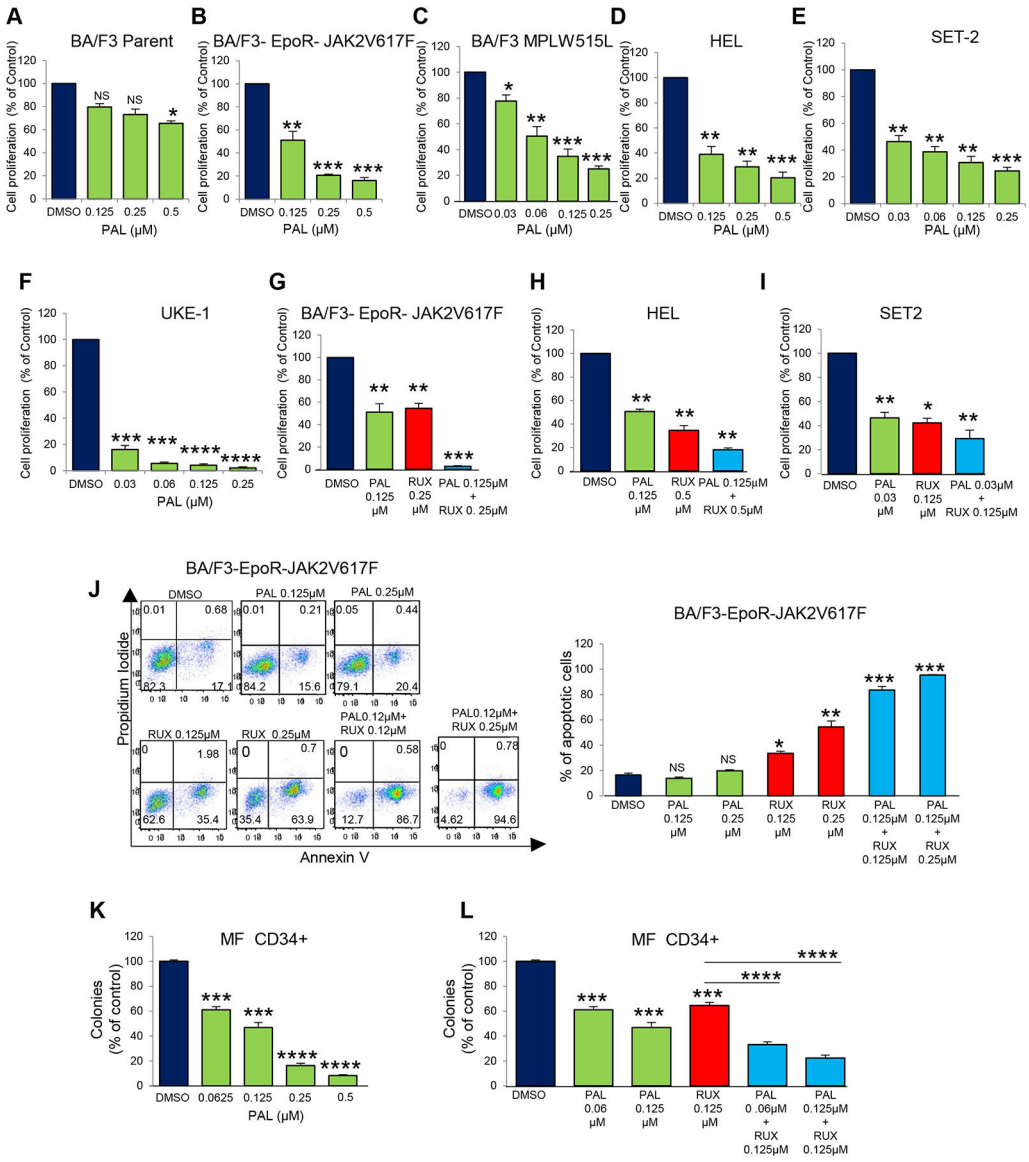

Figure 2. Effects of Palbociclib alone or in combination with Ruxolitinib on hematopoietic cells and progenitors expressing MPN driver mutants.

A-C, BA/F3 (parent), BA/F3-EpoR-JAK2V617F and BA/F3-MPLW515L cells were treated with vehicle (DMSO) or Palbociclib and cell proliferation was assessed by viable cell counts over 5 days. Palbociclib treatment significantly inhibited proliferation of BA/F3-EpoR-JAK2V617F and BA/F3-MPLW515L cells but exhibited modest inhibition of BA/F3 (parent) cells at higher concentration (0.5μM). **D-F,** Palbociclib treatment showed significant reduction in cell proliferation of JAK2V617F-positive human HEL, SET-2 and UKE-1 cells. **G-I,** Combined treatment Palbociclib and Ruxolitinib exhibited significantly greater inhibition of BA/F3-EpoR-JAK2V617F, HEL, and SET-2 cells compared with vehicle or single drug treatment. Values are expressed as percentages of controls (DMSO-treated). Data from three independent experiments are shown in bar graphs as mean ± SEM. **J,** Annexin V/propidium iodide staining followed by flow cytometry was performed to measure apoptosis in BA/F3-EpoR-JAK2V617F cells after treatment with

Palbociclib, Ruxolitinib and Palbociclib/Ruxolitinib combination for 3 days. Representative dot plots of the percentage of apoptotic cells in BA/F3-EpoR-JAK2V617F cells treated with Palbociclib, Ruxolitinib and Palbociclib/Ruxolitinib combination (on the left). Bar graphs showing significant increase in apoptosis of BA/F3-EpoR-JAK2V617F cells by Palbociclib/Ruxolitinib combination treatment. **K,** MF CD34+ cells were plated in complete methylcellulose medium supplemented with cytokines in the presence of DMSO or Palbociclib (0.06– 0.5μM). Palbociclib treatment alone significantly inhibited hematopoietic progenitor colonies in MF CD34+ progenitors (n= 7). **L,** Treatment of Palbociclib in combination with Ruxolitinib exhibited significantly greater inhibition of hematopoietic progenitor colonies in MF CD34+ progenitors compared with single drug treatment (n= 7). Data are represented in bar graphs as mean ± SEM (*p<0.05; **p<0.005, ***p<0.0005; **** p<0.00005; Student's t-test).

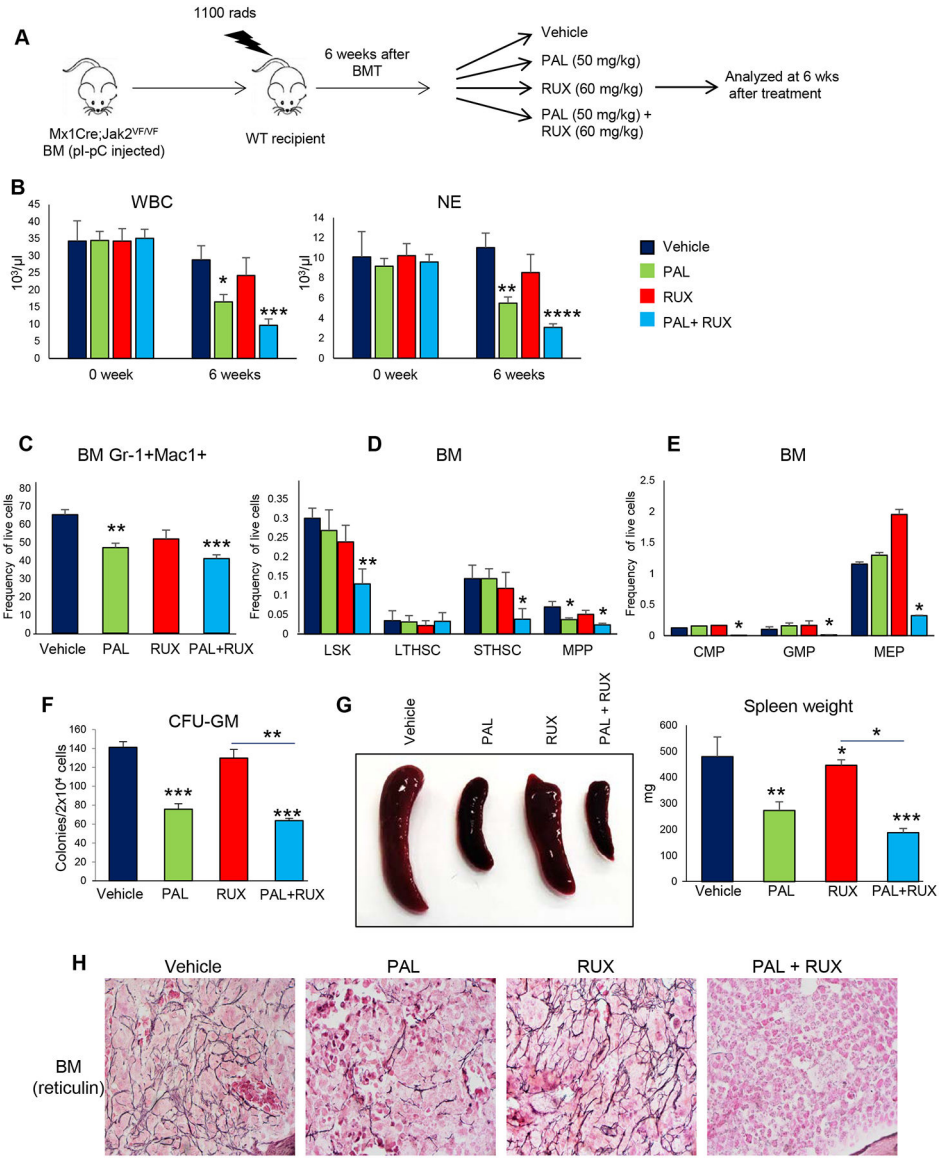

Figure 3. In vivo administration of Palbociclib alone or in combination with Ruxolitinib ameliorates myelofibrosis in Jak2V617F mouse model of MF.

A, Experimental design to assess the in vivo effects of Palbociclib/Ruxolitinib in homozygous Jak2V617F ($Jak2^{VF/VF}$) model of MF. **B,** Peripheral blood WBC and neutrophil (NE) counts were assessed at 6 weeks after treatment (n=8–10). **C,** Frequency of granulocyte/monocyte ($Gr\text{-}1^{+}/Mac\text{-}1^{+}$) precursors in the BM of Palbociclib/Ruxolitinib treated mice is shown in bar graphs as mean ± SEM. **D** and **E,** Flow cytometric analysis of LSK ($Lin^{-}Sca\text{-}1^{+}c\text{-}kit^{+}$), LT-HSC ($Lin^{-}Sca\text{-}1^{+}c\text{-}kit^{+}CD34^{-}CD135^{-}$), ST-HSC ($Lin^{-}Sca\text{-}1^{+}c\text{-}kit^{+}CD34^{+}CD135^{-}$), MPP ($Lin^{-}Sca\text{-}1^{+}c\text{-}kit^{+}CD34^{+}CD135^{+}$), CMP ($Lin^{-}Sca\text{-}1^{-}c\text{-}kit^{+}CD34^{+}Fc\gamma RII/II^{low}$), GMP ($Lin^{-}Sca\text{-}1^{-}c\text{-}kit^{+}CD34^{+}Fc\gamma RII/II^{high}$) and MEP ($Lin^{-}Sca\text{-}1^{-}c\text{-}kit^{+}CD34^{-}Fc\gamma RII/III^{-}$) in the BM are shown in bar graphs as mean ± SEM. **F,** BM cells (2×10^{4}) from $Jak2^{VF/VF}$ mice treated with vehicle, Palbociclib, Ruxolitinib or Palbociclib/Ruxolitinib combination were plated in methylcellulose medium (MethoCult 3434) with cytokines. CFU-GM colonies were scored 7 days after plating.

G, Spleen size/weight in $Jak2^{VF/VF}$ mice treated with vehicle, Palbociclib, Ruxolitinib or Palbociclib/Ruxolitinib combination (n=10–12). (*p<0.05, **p<0.005; and ***p<0.0005; Student's t-test). **H,** Histopathologic analysis. Reticulin staining of the BM sections (X500 magnification) from $Jak2^{VF/VF}$ mice treated with vehicle, Palbociclib, Ruxolitinib or Palbociclib/Ruxolitinib combination. Note that Palbociclib treatment significantly reduced BM fibrosis while combined treatment of Palbociclib/Ruxolitinib almost completely ablated BM fibrosis in $Jak2^{VF/VF}$ mice.

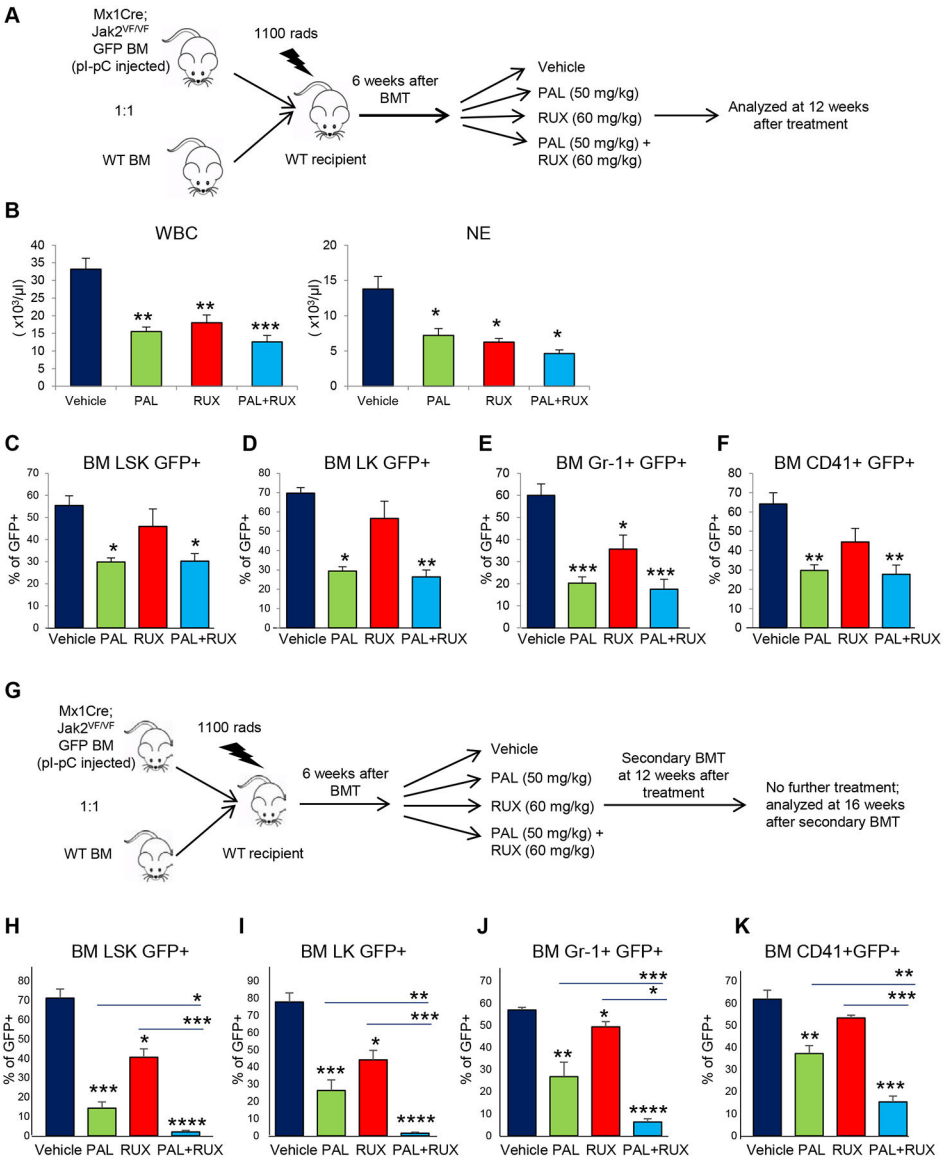

Figure 4. Palbociclib treatment alone or in combination with Ruxolitinib preferentially inhibits Jak2V617F mutant hematopoietic progenitors.

A, Scheme on competitive BM transplantation approach to assess the effects of Palbociclib/Ruxolitinib on Jak2V617F mutant hematopoietic progenitors is depicted. BM cells (5×10^5) from Mx1Cre; $Jak2^{VF/VF}$; GFP mice (6 weeks after pI-pC injection) was mixed with WT C57BL/6 mice BM (5×10^5) at a 1:1 ratio and transplanted into lethally irradiated WT C57BL/6 recipient mice. Six weeks after BMT, recipient mice were randomized to receive treatment with vehicle, Palbociclib (50mg/kg), Ruxolitinib (60mg/kg) or Palbociclib (50mg/kg) and Ruxolitinib (60mg/kg). Drug was administered orally once daily for 12 weeks. **B,** Peripheral blood WBC and neutrophil (NE) counts were assessed at 12 weeks after treatment (n=5). **C-F,** Percentages of $Jak2^{V617F}$ mutant GFP+ LSK ($Lin^-Sca\text{-}1^+c\text{-}kit^+$), GFP+ LK ($Lin^-c\text{-}kit^+$), GFP+ Gr-$1^+$ and GFP+$CD41^+$ cells in the BM of chimeric animals at 12 weeks after treatment are shown; bar graphs represent mean ± SEM (n=5). **G,** Experimental design to assess the effects of drug withdrawal in secondary transplanted

animals. After treatment of chimeric mice with vehicle, Palbociclib (50mg/kg), Ruxolitinib (60mg/kg) or Palbociclib (50mg/kg) and Ruxolitinib (60mg/kg) combination for 12 weeks, BM cells (1×10^6) were transplanted into WT C57BL/6 secondary recipient mice. No treatment was given to secondary recipient animals and they were analyzed at 16 weeks after transplantation. **H-K,** Percentages of $Jak2^{V617F}$ mutant GFP+ LSK, GFP+ LK, GFP+ Gr-1^+ and GFP+$CD41^+$ cells in the BM of secondary recipient animals at 16 weeks after BMT are shown (n= 5 in each group). Data are represented in bar graphs as mean ± SEM (*p<0.05; **p<0.005, ***p<0.0005; **** p<0.00005; Student's t-test).

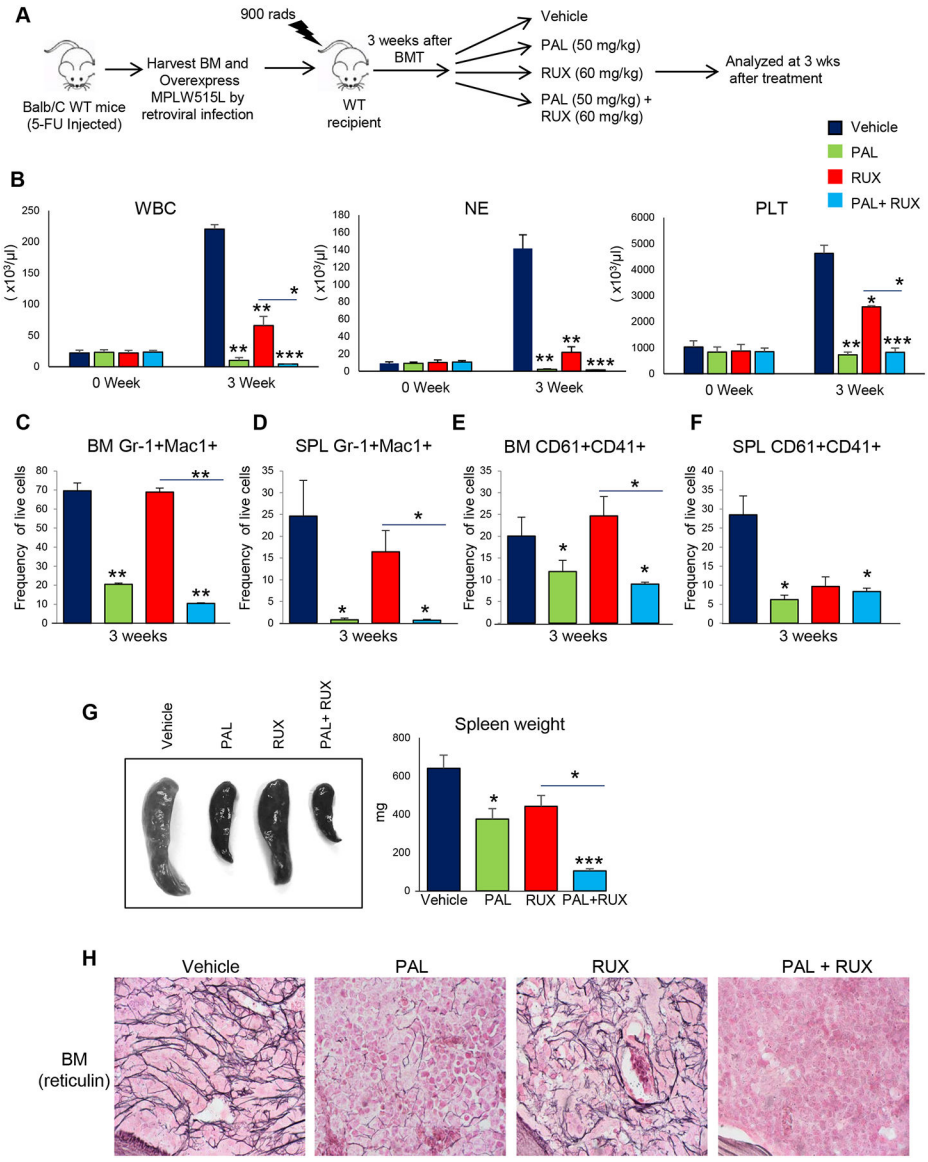

Figure 5. Palbociclib alone or in combination with Ruxolitinib significantly reduces myelofibrosis in MPLW515L mouse model.

A, Experimental design to test the efficacy of Palbociclib/Ruxolitinib in MPLW515L mouse model of MF. **B,** Peripheral blood WBC, neutrophil (NE) and platelet (PLT) counts in the peripheral blood were assessed at 3 weeks after treatment (n=5–9). Data are shown in bar graphs as mean ± SEM. **C-F,** Frequency of granulocyte/monocyte (Gr-1$^+$/Mac-1$^+$) precursors and megakaryocytic precursors (CD61$^+$/CD41$^+$) in the BM and spleens of MPLW515L mice treated with vehicle, Palbociclib, Ruxolitinib and Palbociclib/Ruxolitinib combination is shown in bar graphs as mean ± SEM (n=5). **G,** Spleen size/weight in MPLW515L mice treated with vehicle, Palbociclib, Ruxolitinib and Palbociclib/Ruxolitinib combination (n= 5–9). Data are represented in bar graphs as mean ± SEM (*p<0.05; **p<0.005, ***p<0.0005; Student's t-test). **H,** Histopathologic analysis. Reticulin staining showing extensive fibrosis (grade 2–3) in the BM of vehicle-treated or Ruxolitinib-treated MPLW515L mice. Palbociclib-treated MPLW515L mice BM showed marked reduction in

fibrosis whereas combined treatment of Palbociclib/Ruxolitinib almost completely ablated fibrosis in the BM of MPLW515L mice.

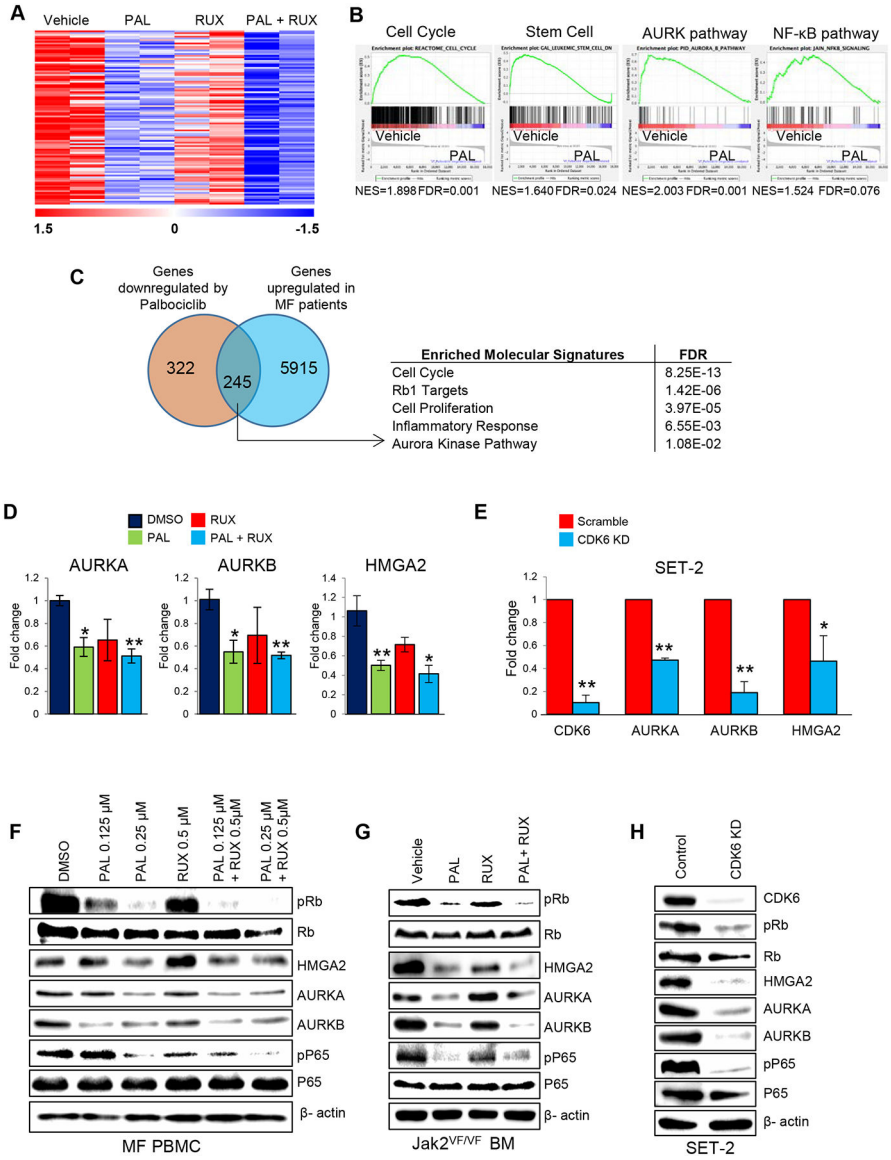

Figure 6. Inhibition of CDK6 by Palbociclib alters gene expression and cell signaling in hematopoietic progenitors expressing Jak2V617F.

A, Heat map showing top 100 significantly downregulated genes (p<0.05, −1.5-fold) in Palbociclib, Ruxolitinib and Palbociclib/Ruxolitinib treated Jak2$^{VF/VF}$ mice LSK (Lin^{-}Sca-1^{+}c-kit^{+}) cells compared with vehicle treated LSK cells. **B,** Gene-set enrichment analyses (GSEA) of the RNA-sequencing data from Palbociclib-treated Jak2$^{VF/VF}$ mice LSK cells compared with vehicle treated Jak2$^{VF/VF}$ mice LSK. Enrichment plots of selected gene sets with normalized enrichment score (NES) and false discovery rate (FDR) are shown. **C,** Venn diagram showing the overlap between upregulated genes in MF patients and genes downregulated by Palbociclib treatment in Jak2$^{VF/VF}$ mice LSK cells. The cutoffs were FDR-adjusted p< 0.05. **D,** Relative expression of AURKA, AURKB and HMGA2 mRNA was determined by RT-qPCR in LSK cells obtained from Jak2$^{VF/VF}$ mice treated with vehicle, Palbociclib, Ruxolitinib and Palbociclib/Ruxolitinib combination. Data from four independent experiments are shown in bar graphs as mean ± SEM (*p<0.05,

p<0.005). **E, JAK2V617F-poitive SET-2 cells were transduced with lentiviral CDK6 shRNA or control (scramble shRNA), and the infected cells were selected using puromycin. Relative expression of AURKA, AURKB, and HMGA2 mRNA was assessed by RT-qPCR and normalized with HPRT expression. Data from three independent experiments are shown in bar graphs as mean ± SEM (*p<0.05, **p<0.005). **F,** PBMC obtained from MF patients were treated with DMSO, Palbociclib, Ruxolitinib or Palbociclib/Ruxolitinib combination at indicated concentrations for 6 hours. Immunoblotting was performed using phospho-specific or total antibodies as indicated. Palbociclib treatment reduced the phosphorylation of Rb and p65 subunit of NF-κB, and decreased the expression of HMGA2, AURKA and AURKB in MF PBMC. Combined treatment of Palbociclib with Ruxolitinib caused more pronounced inhibition of phosphorylation or expression of these target proteins. β-Actin was used as a loading control. **G,** BM cells obtained from $Jak2^{VF/VF}$ mice following in vivo treatment with Vehicle, Palbociclib, Ruxolitinib or Palbociclib/Ruxolitinib combination were subjected to immunoblotting using phospho-specific or total antibodies as indicated. **H,** Immunoblot analysis showed reduced phosphorylation of Rb and p65 subunit of NF-κB, and decreased expression of HMGA2, AURKA and AURKB upon CDK6 knockdown in SET-2 cells. β-Actin was used as a loading control.

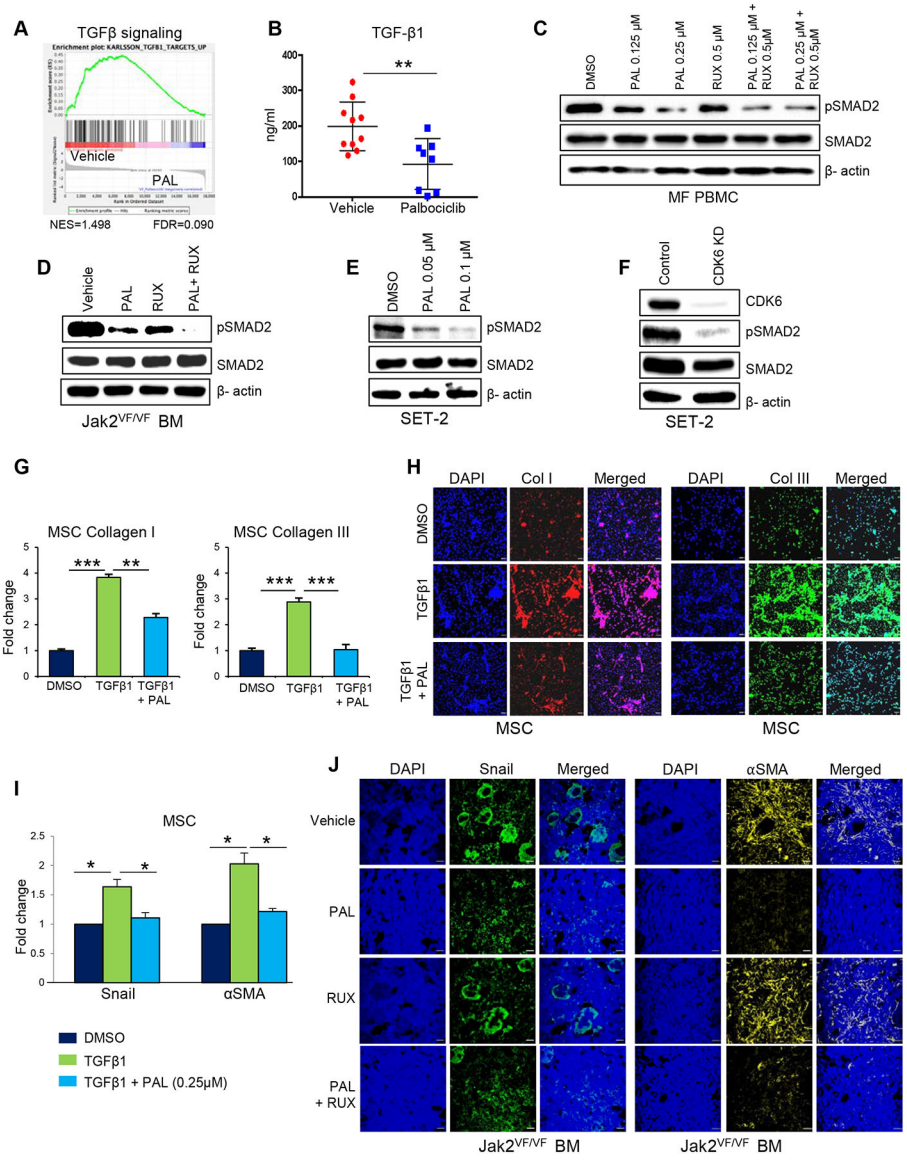

Figure 7. Inhibition of CDK6 by Palbociclib reduces the expression of fibrotic markers.

A, Analysis from the RNA-sequencing data shows downregulation of genes related to TGF-β pathway in Palbociclib-treated Jak2$^{VF/VF}$ mice LSK cells compared with vehicle-treated Jak2$^{VF/VF}$ LSK cells. **B,** Serum TGF-β1 levels in Jak2$^{VF/VF}$ mice treated with vehicle and Palbociclib were assessed by ELISA (n = 8–10) (**p<0.005). **C,** Immunoblot showing decreased phosphorylation of SMAD2 in Palbociclib-treated MF PBMC. Combined treatment of Palbociclib and Ruxolitinib resulted in greater inhibition of SMAD2 phosphorylation. The MF PBMC samples used in Figures 6F and 7C are from the same experiment and the same β-Actin was used as a loading control. **D,** Immunoblot showing decreased phosphorylation of SMAD2 in Palbociclib-treated Jak2$^{VF/VF}$ mice BM. Combined treatment of Palbociclib and Ruxolitinib resulted in greater inhibition of SMAD2 phosphorylation. The Jak2$^{VF/VF}$ mice BM samples used in Figures 6G and 7D are from the same experiment and the same β-Actin was used as a loading control. **E,**

Immunoblot showing decreased phosphorylation of SMAD2 in Palbociclib-treated SET-2 cells. **F,** Knockdown of CDK6 markedly reduced phosphorylation of SMAD2 in SET-2 cells. The SET-2 cell lysates used in Figures 6H and 7F are from the same experiment and the same β-Actin was used as a loading control. **G,** Stimulation with TGF-β1 (50ng/ml) significantly increased Collagen I and Collagen III expression in BM MSC. Treatment of Palbociclib (0.25μM) in presence of TGF-β1 (50ng/ml) significantly reduced Collagen (I and III) expression. The mRNA expression was assessed by RT-qPCR and normalized by Hprt. Data from four independent experiments are shown in bar graphs as mean ± SEM (*p<0.05, **p<0.005). **H,** Immunofluorescence images showing increased expression of Collagen I and Collagen III in MSCs stimulated with TGF-β1 (50ng/ml). Palbociclib (0.25μM) treatment significantly reduced TGF-β1 induced Collagen I and III expression. Collagen I (red), Collagen III (green) and DAPI (blue). **I,** Stimulation with TGF-β1 (50ng/ml) significantly increases Snail1 and αSMA expression in BM MSC. Treatment of Palbociclib (0.25μM) significantly reduced Snail1 and αSMA expression in BM MSC. The mRNA expression was assessed by RT-qPCR and normalized by Hprt. Data from four independent experiments are shown in bar graphs as mean ± SEM (*p<0.05). **J,** Representative immunofluorescence images showing decreased expression of Snail and αSMA in the BM sections of $Jak2^{VF/VF}$ mice treated with Palbociclib alone or in combination with Ruxolitinib. Shown are Snail (green), αSMA (yellow), and DAPI (blue).